Reinforcement in Natural Rubber Elastomer Nanocomposites: Breakdown of Entropic Elasticity

Roberto Peŕez-Aparicio, Arnaud Vieyres, Pierre-Antoine Albouy, Olivier Sanseáu, Loïc Vanel, Didier R Long, Paul Sotta

Reinforcement in Natural Rubber Elastomer Nanocomposites: Breakdown of Entropic Elasticity

Roberto Pérez-Aparicio,[†] Arnaud Vieyres,[†] Pierre-Antoine Albouy,[‡] Olivier Sanséau,[†] Loïc Vanel,[†,§] Didier R. Long,[†] and Paul Sotta*[,†]

[†]Laboratoire Polymères et Matériaux Avancés, CNRS/Solvay, UMR5268, R&I Centre Lyon, 85 avenue des Frères Perret, 69192 Saint Fons Cedex, France

[‡]Laboratoire de Physique des Solides, UMR8502, CNRS/Université Paris-Sud, 91405 Orsay Cedex, France

[§]Institut Lumière Matière, UMR5306, CNRS/Université Lyon 1, 69622 Villeurbanne Cedex, France

ABSTRACT: We propose an approach based on the combination of different techniques in order to discriminate various reinforcement effects in vulcanized natural rubber elastomers with various cross-link densities, filled with carbon black or silica: mechanical response, independent measure-ments of the cross-link density by proton multiple-quantum NMR, and measurements of chain segment orientation under stretching by X-ray scattering. We show that, while the modulus measured in dynamical mechanical measurements decreases as the strain amplitude increases (Payne effect), the response of the elastomer matrix in terms of average chain segment orientation under stretching measured by X-ray scattering stays constant. The amplification of average chain segment orientation is comparable to the amplification of modulus measured at medium/large strain amplitude. By analyzing the deviations with respect to the behavior of the pure unfilled elastomer matrix, we show that the contribution due to strain amplification effects in the elastomer matrix can be selectively distinguished. We show that the mechanical response at medium/large strains is essentially driven by strain amplification effects, while, in the linear regime, there is a strong additional reinforcement which is not related to the properties of the elastomer matrix. Hypothesis on the origin of this additional reinforcement are suggested and discussed.

1. INTRODUCTION

The search for lighter and nevertheless high mechanical performance materials has boosted the use of polymer composite materials in the industry. On the one hand, much progress has been made in the understanding of their mechanical properties based on mainly geometrical and/or structural arguments and the knowledge of the individual properties of the polymer matrix and the solid fillers.[1] On the other hand, in the past decade, there have been increasing evidence that the physical properties of the polymer itself can be strongly modified at the solid interface, especially when considering nanometer scales for which shifts of the polymer glass transition temperature T_g have been reported.[2,3] Such modification of the polymer properties at the molecular level should have a significant impact on the mechanical properties of nanocomposites, and in particular on reinforcement, which can be defined in a heuristic way, e.g., as the ratio R of the elastic modulus of the composite material over that of the pure polymer matrix. However, quantifying the relative contributions of the various physical mechanisms that can explain mechanical reinforcement of nanocomposites remains a true experimental and theoretical challenge.[4]

Elastomers filled with solid particles or aggregates (denoted as fillers) have remarkable mechanical properties, with a rich and complex phenomenology.[5] Carbon black (CB) and/or silica (SIL) aggregates are commonly used as fillers.[6] Efficient reinforcement is obtained with submicrometric or nanometric fillers dispersed down to the scale of elementary aggregates or particles. It has been a challenge to elaborate a unifying picture of the quite diverse but nevertheless related effects occurring in these materials. The primary effect is modulus enhancement in the linear regime, with a marked dependence on the filler morphology, volume fraction, average size, surface treatment and dispersion state. The modulus enhancement, represented as the ratio R defined above, has a marked temperature dependence, with a maximum a little bit above the glass transition temperature T_g of the pure matrix (see Figure 1a). There is usually a large temperature range in which the reinforcement is significantly higher (and sometimes much higher) than predicted by the pure hydrodynamic (or strain amplification) effect, specially at relatively high filler volume fractions. The material toughness, or equivalently energy at break, is also strongly enhanced. Associated to reinforcement is the so-called "Payne effect", that is the large drop of the storage modulus measured in oscillatory strain, together with a peak in loss modulus, as the strain amplitude is increased beyond

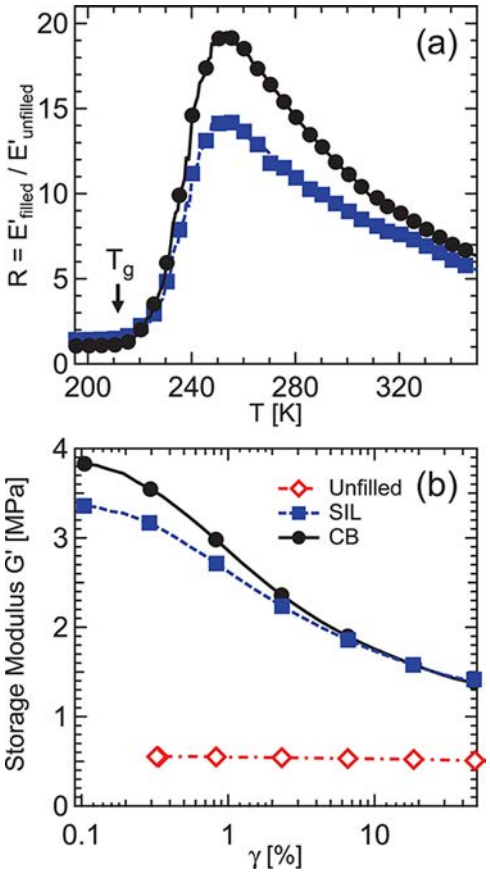

Figure 1. (a) Reinforcement in the linear regime at 10 Hz as a function of temperature and (b) oscillatory shear modulus G' as a function of the strain amplitude γ at 333 K and 10 Hz in unfilled (◊), SIL (■), and CB (●) filled NR samples with 18.25% volume fraction of fillers. All samples have roughly the same cross-link density.

typically 1% to 10% (see Figure 1b).[7] It is important to note that, after some transitory, partly irreversible drop of modulus (the so-called "Mullins effect"), this decrease of the modulus as a function of the strain amplitude (as illustrated in Figure 1b) is reversible. The behavior of un-cross-linked polymer melts is also strongly affected by the presence of solid filler particles. In particular, very long relaxation times appear, eventually resulting in huge modulus enhancement at low frequencies. For the sake of clarity, we shall discuss only cross-linked materials here.

Several approaches, based on different physical mechanisms, have been proposed to explain reinforcement.

In one class of approach, the predominant mechanism relies on filler−matrix interactions at filler surfaces.[8] Chain adsorption would be responsible for an increased density of trapped entanglements around filler particles which would be responsible for the enhanced modulus (beyond the pure hydrodynamic effect) in the linear regime. In this approach, the mechanical response is essentially driven by the properties of the elastomer matrix alone. Studies have been performed with polymer chains of different molecular weights and fillers with different surface treatments to vary the density of trapped entanglements.[8] In particular, below the filler percolation threshold, reinforcement thus would come from parts in the matrix in which elastomer chains are subjected to very high local strains and/or an increased density of effectively active constraints (cross-links and entanglements) in the vicinity of filler particles, due to trapping effects associated with adsorption of chains on the filler surfaces.[9−12] Then, a significant fraction of the chains might contribute to modulus enhancement at large strain amplitude due to finite chain extensibility.[8]

These trapped entanglements would be released due to chain desorption upon applying a large amplitude strain, which would explain the drop of the modulus. Indeed, there has been a number of studies which show that reinforcement is affected by the polymer molecular mass and is particularly pronounced when distances between fillers are comparable to or larger than the size of the chains, which very roughly corresponds to the thickness over which the density of trapped entanglements would be increased around the fillers.[8,9]

On the other hand, nonlinear effects and dissipative properties have been explained by desorption/absorption of polymer chains at filler surface,[13] leading to disentanglement of bulk rubber matrix from bounded chains.[14]

However, there has been no direct experimental evidence of an increased density of entanglements close to filler particle surfaces, nor of disentanglements under the effect of large amplitude strain. Interpretations were based on careful analysis of mechanical experiments, in which the response of the whole material is measured, with contributions coming from the matrix, fillers and interfaces. Molecular dynamics simulations show that the entanglement density may be increased in the vicinity of an adsorbing surface.[15] Monte Carlo simulations of chain wrapping around fillers and disentanglement under large amplitude strain have been performed.[16]

Another mechanism which has been put forward is filler agglomeration and percolation, resulting in filler networking.[17] In such a picture, the large enhancement of the modulus is related to the transmission of the stress through the filler network. Indeed, it is generally observed that the modulus starts to deviate from the pure hydrodynamic prediction and increase quite abruptly above a critical volume fraction, which depends on the type of fillers. Breaking down such a filler network and/or particle reorganization under large amplitude strain, leading to destruction/reformation of the filler network, would then lead to the observed nonlinear drop of the modulus.[1,7,18,19]

Note that in both approaches, a fraction of the matrix (occluded rubber and an adsorbed, immobilized elastomer layer[20]), may contribute to the undeformable fraction of the sample.

In yet another class of approach, it has been claimed that the behavior of the elastomer matrix itself is strongly modified by the presence of glassy domains due to a T_g shift of the matrix in the vicinity of fillers.[21−24] It is based on the fact that, even though the above mechanisms may play a role in the higher temperature range, they can certainly not explain the very large maximum of reinforcement R (up to R = 30 at 20 vol % filler typically) a bit above the elastomer matrix T_g. On the basis of measurements on well-defined model systems, the reinforcement, including the nonlinear elastic and dissipative responses, could be successfully modeled by considering an effective solid fraction including a rigid (glassy) polymer around filler particles,[22,25,26] as measured directly by NMR, and forming glassy bridges. Direct experimental evidence for glassy layers are very difficult to obtain, mostly because a small fraction of the polymer may eventually be affected. One needs to work on very clean model systems to be able to observe such a small fraction of the matrix. The subject is still under active debate.

The relative contribution of the various mechanisms mentionned above may be very different in different circumstances, depending on material parameters (matrix cross-linking, filler system) and on test conditions (essentially strain amplitude, strain rate and temperature). Indeed, it has been claimed that glassy bridges may not be the dominant mechanism in little reinforced systems and/or at temperatures very far above the T_g of the matrix.[27,28]

The above discussion indicates that it is still a major issue to gain selective information on the various mechanisms contributing to reinforcement in filled polymer melts and filled elastomers. Note also that the order of magnitude of the reinforcement which can be provided by the various mechanisms has been often overlooked.

In a recent paper, we have introduced a new combination of techniques, in particular mechanical experiments (uniaxial stretching) combined with in situ X-ray scattering measurements of chain segment orientation and careful measurements of cross-link densities.[29] In a series of unfilled natural rubber networks with different levels of cross-linking, we have shown that characterizing segmental orientation allows obtaining a detailed picture of cross-linking and entanglement effects. We have been claiming that extending this approach to filled materials may allow one to get some new insight on reinforcement mechanisms. This is the purpose of the present work. We propose to investigate selectively the behavior of the elastomer matrix in filled systems with this approach.

The proposed approach is based on the very general law which directly relates the elastic stress in a rubber to network chain segment orientation. This relationship is the basis of rubber elasticity and has been shown to be valid in elastomers and cross-linked gels.[30,31] Here we argue that some conclusions can be drawn on reinforcement mechanisms from checking its validity in reinforced materials.

As regards the nonlinear behavior observed in large amplitude oscillatory strain experiments (Payne effect), a topic which has received a growing interest from the scientific community,[32] it has been generally considered that at higher strain, beyond filler network breakup, the reinforcement mechanism is primarily local strain amplification. Concerning reinforcement, the similarity of the problems of a suspension of particles in a viscous fluid and of a dispersion of particles in an incompressible elastic solid has been recognized long ago.[33,34] Considerable progress has been made recently on the analysis of local strain amplification in a filled polymer matrix.[35] The so-called "hydrodynamic amplification factor" is expressed as the ratio of the viscosity of the composite over that of the pure matrix (in the case of a viscous liquid or melt), or similarly as the ratio of the shear storage moduli of the composite over that of the pure matrix (in the case of an elastic matrix). The strain amplification factor is expressed as the average strain rate (in a viscous fluid or melt) or strain (in an elastomer) over that in the pure matrix. It is shown in Domurath et al. that the expressions for both quantities are different on a very general basis.[35] Note that the derived expressions hold in the linear regime. Our experiments shed a new light on this point by providing a direct experimental evidence of strain amplification effects at large strain.

The paper is organized as follows. In section 2, we explain the background of the general approach which has been developed, based on a combination of different techniques. We describe the studied materials and experimental techniques in section 3. Results are presented in section 4 and discussed in section 5.

2. GENERAL APPROACH

2.1. Background. The approach introduced here is based on the selective observation of the behavior of the elastomer matrix. The basic theory of rubber elasticity is based on the very general law[36]

$$\sigma_{ij} = (3k_BT/b^3)\langle u_i u_j - \delta_{ij}/3\rangle \tag{1}$$

where σ_{ij} is the stress tensor, u_i the ith component of the unit vector $\vec{u}$ tangent to a polymer chain (brackets denote statistical averaging), and b^3 the volume of a statistical segment. This is valid even in the nonlinear regime and expresses that the physical origin of the stress is entropic, being related to chain configurational statistics, or equivalently to chain segment ordering, under an applied strain. In the particular case of uniaxial extension, eq 1 transforms into the well-known stress-optical law

$$\sigma = \frac{k_BT}{b^3}\langle P_2(\cos\theta)\rangle \tag{2}$$

where the segmental orientation order parameter $\langle P_2(\cos\theta)\rangle$ is the average of the second order Legendre polynomial $(3\cos^2\theta - 1)/2$, with θ the angle between any chain segment and the direction of the strain.

On the basis of classical assumptions on the network structure, *in the linear regime*, the average segmental orientation $\langle P_2(\cos\theta)\rangle$) can then be expressed as a function of the stretch ratio $\lambda = L/L_0$

$$\langle P_2(\cos\theta)\rangle = b^3\nu\psi(\lambda^2 - \lambda^{-1}) \tag{3}$$

where ν is the cross-link number density (in m^{-3}) and ψ a factor which depends on cross-link functionality and displacement under strain: for a tetrafunctional, phantom network model, ν is half the number density of elastic chains and $\psi = 1$.[31] Combining eqs 2 and 3, one gets a shear modulus $G' = k_BT\nu\psi$. For usual densities of about one cross-link per 100 monomers, G' is about 5×10^5 Pa and would extrapolate to about 10^7 Pa at an (unphysical) maximum cross-link density of one cross-link per monomer.

Note that, in an inhomogeneous (still unfilled) rubber material, heterogeneity of the local strain or stress may come from heterogeneities of the cross-link density, resulting in an inhomogeneous rubbery modulus. The local stress σ_{ij} varies in space and is still given locally by eq 1. Then, eq 1 (or eq 2 in the case of a unaxial tensile test) should remain valid globally upon volume integration.

Entropic rubber elasticity is very distinct from intermolecular forces acting in a glassy polymer, which give a shear modulus of order 10^9 Pa, that is 2 orders of magnitude larger. Equation 1 corresponds to an ideal situation in which enthalpic contributions associated with intramolecular interactions would be completely negligible.[31,37] This is generally not true. Specifically, in natural rubber, the nonentropic contribution represents a fraction of 0.12−0.19 (according to the various thermodynamical ways of measuring it) of the total elastic free energy.[31] This rather large contribution is basically due to the effect of chain stretching on the distribution of gauche and trans rotamers, which have different energies.

It is not our purpose to discuss this point (specifically the temperature variation of the modulus of unfilled systems in the

high temperature range) in details here. We shall rather proceed by comparing the behavior of filled materials to their pure (unfilled) counterparts, based on our previous characterization of the pure unfilled materials.[29] The cross-link density is used as control parameter. It was shown that the chain segment orientation (as measured from X-ray scattering) is indeed proportional to the elongation function $\lambda^2 - \lambda^{-1}$ (eq 3) up to very high extensions, and also to the stress (in a more limited range of extensions however), with an initial slope independent of the cross-link density, in agreement with eq 2. Thus, we consider the set of curves which have been obtained in pure (unfilled) systems as a reference for the behavior of the elastomer matrix. This linear relationship between the elongation function and segmental orientation is a constitutive law for the considered matrix.

In an elastomer material reinforced by fillers, the constitutive relationship between strain and segmental orientation (eq 3) may be used to probe selectively the strain within the elastomer matrix, by measuring the average segmental orientation during uniaxial stretching experiments. Then, by measuring the overall mechanical response (the stress) during the same experiments, it is possible to discriminate which part of the stress may be attributed to strain amplification in the matrix. By performing experiments in a wide range of strain amplitudes, it may be checked how the part of the stress which is due to strain amplification depends on the strain amplitude.

The various possible contributions to the stress in a filled material may be discussed as follows. A plane P within the sample (Figure 2a) can be divided into surface elements dS

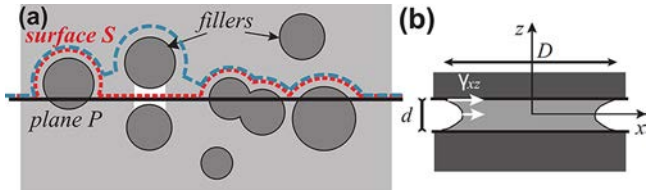

Figure 2. (a) In a material with non percolating fillers, the total force through the plane P (line) may be computed across a surface S (blue dashed curve) going only through the elastomer matrix. When fillers percolate through direct contact or rigid polymer bridges (schematized as the white region), the surface S necessarily crosses the rigid network (red dotted curve). (b) In a thin layer confined between two filler surfaces, strong shear strains γ_{xz} appear upon applying a tensile strain γ_z.

(large with respect to the monomer size) in which the local stress σ_{ij} may be entropic (rubbery surface element, index (e) in eq 4) or nonentropic when P crosses a solid filler (index (f)). We suppose also that the response of the elastomer matrix may be strongly affected and become solid-like (rigid or glassy) in some strongly confined regions (index (g)), as schematized by the white zone in Figure 2a. The total force through the plane is:

$$F_i = \int_{(e)} \sigma_{ij}\, \mathrm{d}S_j + \int_{(g)} \sigma_{ij}\, \mathrm{d}S_j + \int_{(f)} \sigma_{ij}\, \mathrm{d}S_j \qquad (4)$$

Different situations may occur. In case the filler network does not percolate (or has been broken by applying a large amplitude strain), when a filler intersects the plane, the force F_i can be equivalently computed by integrating along a surface S moved away from the filler surface, which goes only through the elastomer matrix (as schematized by the blue surface in Figure 2a). In this case, the local stress obeys eq 3 through the whole surface and the overall (macroscopic) stress is still given by eq 1, integrating along the surface S. On the other hand, if fillers percolate, either by direct contact or through regions in which the local response of the polymer is rigid (schematized by the white zone in Figure 2a), the surface S cannot be drawn entirely through the elastomer matrix . In this case, the force will be given by:

$$F_i = \frac{3k_BT}{b^3} \int_{(e)} \langle u_i u_j - \delta_{ij}/3 \rangle\, \mathrm{d}S_j + \int_{(g)} \sigma_{ij}\, \mathrm{d}S_j \qquad (5)$$

and contains some *nonentropic* contributions (term with index (g)).

There is yet another possible contribution to the mechanical response in thin layers confined between filler surfaces. Let us consider the case of strong confinement, that is, a thin elastomer layer confined between filler surfaces, such that the layer thickness d is small compared to the lateral dimension D of the confining surfaces, and with no slip at surfaces (Figure 2b). Because of the nonslip condition at surfaces, imposing a tensile stress ϵ (along z) to the layer results in a very large shear strain $\gamma_{xz} \approx a\epsilon$ with $a = D/d \gg 1$ a local strain amplification factor, which will contribute to the elastic energy density by a term of order $\Delta F \approx G' a^2 \epsilon^2$ where G' is the shear (elastomeric) modulus, leading to an effective modulus of order $G'a^2 \gg G'$.[38] This situation is analogous to lubrication flow.[39,40] To our knowledge, the corresponding contribution to reinforcement in polymer nanocomposites has not yet been explicitly discussed. As regards segmental orientation, since only the component $\langle u_z u_z \rangle$ is measured (other components being averaged to zero by symmetry arguments), it occurs that overall entropic elasticity breaks down in this case as well, the stress being amplified by a factor a as compared to the average segmental orientation parameter $\langle P_2 \rangle$. Note that, depending on lateral boundary conditions, a local hydrostatic pressure may also be induced, resulting in an additional nonentropic contribution to the stress involving the bulk modulus,[41] which is much larger (typically 3 orders of magnitude larger) than the shear modulus.

Thus, the general law (eq 3) shall be recovered macroscopically if the whole matrix has locally an entropic response, without any contribution from glassy or strongly confined parts (extra term with index (g) in eq 5). Conversely, violation of eq 3 in a reinforced material would imply that the stress is not related to the properties of the elastomer matrix only and contains some contribution from percolating, solid or strongly confined parts of the elastomer matrix. Therefore, checking whether eq 3 remains valid macroscopically in reinforced (filled) elastomer materials allows to discriminate the purely entropic contribution to the mechanical response (this is the part measured through average segmental orientation) from the nonentropic contributions originating from direct filler−filler contacts, glassy bridges or strongly confined layers. It may thus provide direct experimental discrimination of entropic and nonentropic reinforcement mechanisms.

2.2. Experimental Approach. Here we propose an innovative experimental approach in which the various quantities in eqs 1 and 3, i.e., the stress σ and the segmental orientation order parameter $\langle P_2(\cos\,\theta) \rangle$, are measured independently and selectively in reinforced elastomer systems. Referring to the behavior of pure, unfilled elastomer matrices, in which the relationships contained in eq 3 are effectively

established,[29] deviations observed in reinforced materials are analyzed.

In a uniaxially stretched elastomer network, the distribution of chain segments becomes anisotropic, with more (respectively less) segments oriented parallel (respectively perpendicular) to the stretching direction. From this induced anisotropy of the orientational distribution of chain segments, a segmental orientation order parameter $\langle P_2(\cos\theta)\rangle$ may be defined as an ensemble average over all segments in the elastomer matrix. Because of this induced average segmental orientation, the amorphous X-ray scattering halo becomes anisotropic, with more (less) intensity in the direction perpendicular (parallel) to the stretching direction. The segmental orientation order parameter $\langle P_2(\cos\theta)\rangle$ may be directly measured from the observed anisotropy, with a constant proportionality factor (not calibrated here) related only to the atomic structure of monomers.[42,43]

Cross-link densities ν in the elastomer matrices are measured in both pure and reinforced materials by proton Multiple-Quantum (MQ) NMR experiments,[44] in which residual dipolar couplings between protons, partially averaged under the effect of the restriction on chain segment reorientation due to cross-links and entanglements,[45] are determined quantitatively. For each chain, a nonzero dynamical average is obtained, with an angular part (dependent upon the local orientation of the chain) and a magnitude, dependent upon the local degree of stretching. When averaged over the ensemble of polymer chains, the local anisotropy of orientational motions may be described by a nonzero dynamical average $\overline{P}_2$ of the second order Legendre polynomial for the polymer backbone orientation. In other words, in NMR, *individual* chain segment orientation is measured and its magnitude then averaged over all network chains. The dynamical average $\overline{P}_2$ gives directly the average cross-link density ν with a proportionality factor which has been numerically calibrated.[46]

The overall NMR signal is the superposition (sum) of contributions from all regions in the matrix where the cross-link density may be considered to be homogeneous. The overall average cross-link density ν is obtained with high accuracy.[46] Moreover, cross-link density distributions are obtained by suitable data analysis.[44,46,47]

It is important to emphasize once again that $\overline{P}_2$ and $\langle P_2(\cos\theta)\rangle$ are distinct quantities. $\overline{P}_2$ is a dynamical average measured by NMR in the *relaxed state*, whereas $\langle P_2(\cos\theta)\rangle$ is an overall (ensemble) average anisotropy, which is zero in an isotropic system (that is, in the relaxed state) and becomes nonzero under stretching only. At high temperature (so that local reorientational motions are fast) both quantities are functions of the cross-link density through arguments based on chain statistics in rubber elasticity theory.

3. MATERIALS AND TECHNIQUES

The investigated elastomers are *cis*-1,4 polyisoprene (natural rubber (NR) of grade SMR 5L with DSC measured T_g = 213 K) reinforced with 18.25 vol % of (i) precipitated silica (SIL samples, Z1165MP from Solvay, 160 m^2/g) treated with bis(triethoxysilylpropyl)-tetrasulfane (TESPT), which provides covalent silica/elastomer coupling; and (ii) carbon black (CB samples, N234 from Cabot, 120 m^2/g). Samples were mixed and sulfur vulcanized following standard procedures. The mixing procedure consisted of one phase in an internal mixer during which rubber, fillers, TESPT (in case of silica fillers), vulcanization activators (4 g of ZnO and 2 g of stearic acid per 100 g of rubber) and an oxidation preventor were blended. Curing agents (sulfur (S)) and accelerators (*N*-cyclohexyl-2-benzothiazole-sulfenamide (CBS) and 0.2 g of tetrabenzylthiuram disulfide (TBzDT)) were added on an open roll mill at low temperature to avoid premature cross-linking. Three CB and three SIL samples with different cross-link densities ν were prepared by changing the sulfur (S) content between 0.5 and 2.5 wt %, with a constant ratio CBS/S = 1.3 (for SIL samples) or CBS/S = 1.0 (for CB samples), CBS being the primary vulcanization accelerator. Moreover, a set of six pure (unfilled) NR samples with different cross-link densities prepared in similar conditions were used for comparison.[29] The main formulation ingredients of all studied samples are summarized in Table 1.

Table 1. List of the Studied Samples[a]

denomination	NR	SiO_2	CB	S	CBS
unfilled	100			0.5	0.66
	100			1.0	1.33
	100			1.5	2.0
	100			1.5	2.0
	100			2.0	2.66
	100			2.5	3.33
SIL	100	50		0.5	0.66
	100	50		1.5	2.0
	100	50		2.5	3.33
CB	100		45	0.5	0.5
	100		45	1.5	1.5
	100		45	2.5	2.5

[a]NR denotes natural rubber SMR 5L, SiO_2 denotes Z1165MP silica, CB denotes N234 carbon black. S is the sulfur and CBS the accelerator. All amounts are expressed in phr (g per 100 g of rubber).

Proton MQ NMR experiments were carried out at 343 K (that is, well above T_g) on a Bruker minispec mq20 spectrometer operating at 0.5 T with 90° pulses of down to 2 μs and a dead time of 15 μs. Well established procedures were used to obtain and analyze the normalized proton double quantum (DQ) signals in order to obtain the distribution of cross-link densities in all studied samples.[44] Oscillatory shear moduli G^* were measured in as-prepared samples (thickness 2 mm) at 333 K and frequency 10 Hz on a Metravib VA 3000 DMA. Sweeps of shear amplitude γ increasing from 0.1% up to 50% and then decreasing back to 0.1% were applied. Storage moduli G' were measured during the return sweeps. Average chain segment orientation under tensile strain was measured at 298 K with a homemade uniaxial stretching device mounted on a rotating anode X-ray generator, described in details elsewhere.[29,43] The true stretch ratio $\lambda = L/L_0$ at X-ray beam spot is measured simultaneously both with an optical camera and using the variation of sample thickness measured through the variation of X-ray absorption. 2D scattering patterns were recorded in samples stretched in situ as a function of λ and the anisotropic intensity in the amorphous halo (with more (respectively less) intensity in direction perpendicular (respectively parallel) to the stretching direction) was fitted as a function of the azimuthal angle φ with the expression $A + B\cos^2\varphi$ (where A is corrected for air scattering). The anisotropy of the scattered intensity may be characterized by a parameter $\langle P_2\rangle_{RX} = 2B/(15A + 10B)$, which, as quoted above, is proportional to $\langle P_2(\cos\theta)\rangle$.[29,43]

The dispersion states of the fillers were characterized by electron microscopy and small angle scattering experiments. Representative TEM and SEM micrographs of the same silica-filled samples were shown in ref 48.

4. RESULTS

Reinforcement curves as a function of temperature are shown in Figure 1a for CB and SIL samples with roughly the same cross-link densities (samples with 1.5 phs S normalized by the pure matrix with 1.0 phr S, cross-link densities are reported in abscissa in Figure 3). The drop of the G' modulus in the range γ = 0.1−50% is shown in Figure 1b for CB and SIL samples

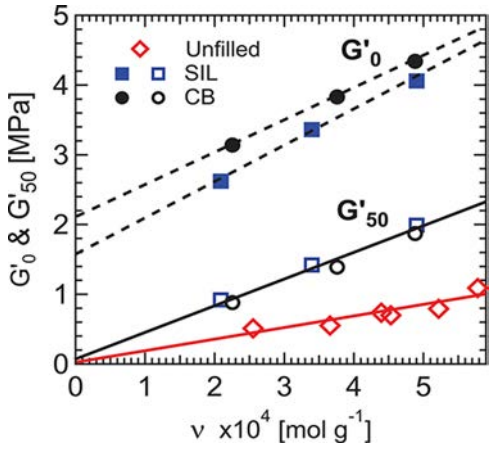

Figure 3. Storage shear moduli G'_0 (full symbols) and G'_{50} (empty symbols) for the 12 different studied samples, as a function of the cross-link density ν measured by NMR: unfilled (◊), SIL (□), and CB (○) samples.

with same cross-link densities. The modulus of a pure, unfilled sample, also shown in Figure 1b, is roughly constant in this range. Storage moduli at strain amplitudes 0.1% (G'_0) and 50% (G'_{50}) are shown in Figure 3 as a function of the average cross-link density ν (measured by NMR). In unfilled systems, the modulus is proportional to the cross-link density and extrapolates to nearly zero modulus at $\nu = 0$, which indicates that roughly the same amount of effective (physical and chemical) cross-links are detected in both NMR and mechanics, in this range of strain amplitudes.[29] The slope of G' vs ν (1.7×10^9 Pa g mol^{-1}) corresponds almost quantitatively to the prediction of eq 3 (2.4×10^9 Pa g mol^{-1}). In reinforced systems, the values of G'_{50} are still proportional to the cross-link density, with a slope about twice as large however (i.e., with a constant reinforcement factor of about two). Conversely, G'_0 is not proportional to ν. Thus, we argue that different mechanisms may be involved in reinforcement at very small strain amplitudes (linear regime, γ = 0.1%) and at intermediate/large amplitudes (γ = 50%).

The curves of $\langle P_2 \rangle_{RX}$ vs the elongation function $\lambda^2 - \lambda^{-1}$ are shown in Figure 4a for three pure and reinforced systems with similar cross-link densities. Above the onsets of strain-induced crystallization (SIC, indicated by arrows), unfilled systems show a roughly constant orientation of the amorphous phase in equilibrium with crystallites,[43] while in filled materials $\langle P_2 \rangle_{RX}$ further increases due to a more inhomogeneous crystallization process. Below the onsets, $\langle P_2 \rangle_{RX}$ varies linearly with $\lambda^2 - \lambda^{-1}$ in a wide range of strain values (from 0% up to 250% in unfilled, from roughly 15% up to 120% in filled materials) in agreement with eq 3. The slightly nonzero intercepts of the curves at $\lambda^2 - \lambda^{-1} = 0$ correspond to experimental background. The $\langle P_2 \rangle_{RX}$ curves stay perfectly linear down to $\lambda^2 - \lambda^{-1} = 0$. Interestingly, prior to crystallization onsets, $\langle P_2 \rangle_{RX}$ curves do not show any significant upward deviation related to finite chain extensibility, either for the pure or the filled materials.

The slopes S_2 of $\langle P_2 \rangle_{RX}$ vs the elongation function $\lambda^2 - \lambda^{-1}$ are shown as a function of ν for all systems in Figure 4b. In all systems, S_2 shows an excellent linear correlation with ν (as predicted by eq 3), with a nonzero intercept at origin however. This nonzero intercept corresponds to effective constraints (entanglements) detected by NMR in addition to chemical cross-links and not detected in X-ray measurements, due to the

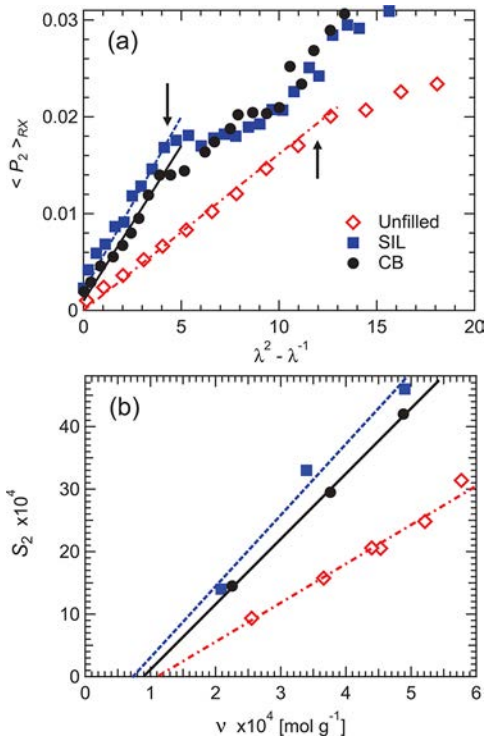

Figure 4. (a) Amorphous orientation parameter $\langle P_2 \rangle_{RX}$ measured by X-ray scattering as a function of the elongation function $\lambda^2 - \lambda^{-1}$ for systems with the same cross-link density: unfilled (◊), SIL (■), and CB (●) samples. Crystallization onsets are indicated by arrows. (b) Slopes S_2 of $\langle P_2 \rangle_{RX}$ as a function of the cross-link density ν measured by NMR.

different characteristic frequencies, since X-rays experiments are done under quasi-static mechanical loading. This means that the measured value of S_2 may effectively be zero when extrapolated to zero chemical cross-link (i.e., in the molten state). It indicates that part of the constraints which are effective on the time scales of NMR experiments (of order 10 kHz) and in dynamical mechanical measurements (10 Hz) may relax on longer time scales. Note also that X-rays measurements involve medium to large strain values while NMR experiments are done in the relaxed state.

To further illustrate the strong deviation between the mechanical response and the segmental orientational response, both the storage moduli G' and S_2 slopes are plotted as a function of the elongation function $\lambda^2 - \lambda^{-1}$ in Figure 5 for a representative pair of samples, after being normalized by the corresponding values obtained in the pure system with the same cross-link density. SIL and CB samples with 1.5 phr sulfur have been used, data are normalized with the unfilled sample with 1.0 phr sulfur, which has roughly the same cross-link density (see Figure 3). For the segmental orientational response S_2, constant values corresponding to the slopes in Figure 4a have been reported. This figure is only another way of representing the difference between the mechanical response and the segmental orientational response. It shows explicitly that, while the modulus measured in dynamical mechanical measurements decreases as the strain amplitude increases (Payne effect), the response of the elastomer matrix in terms of average chain segment orientation under stretching measured by X-ray scattering stays constant.

In reinforced materials, the amorphous phase orientation is increased by a roughly constant proportionality factor (of order

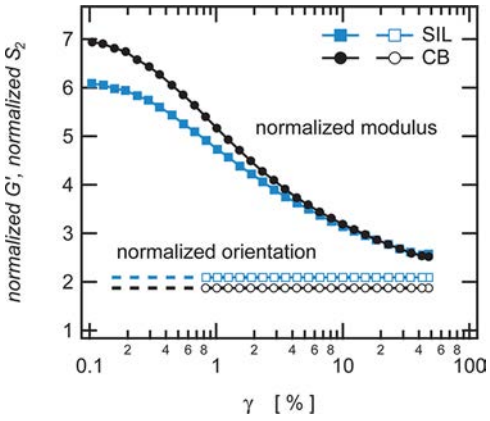

Figure 5. Storage shear moduli (full symbols) and slopes of the segmental orientation S_2 (empty symbols) as a function of the tensile strain for two representative samples (■, SIL; ●, CB), normalized by the corresponding values in the unfilled sample with the same cross-link density. For the normalized moduli, γ is the amplitude of the oscillatory strain, for the normalized slopes, $\gamma = \lambda - 1$.

1.8 for CB and 2 for SIL) with respect to an unfilled system with the same cross-link density. This factor corresponds almost quantitatively to the reinforcement factor observed for G'_{50} (or equivalently for the stress in the 50% strain amplitude range) in Figure 3.

Thus, relating local chain segment orientation to local strain, according to eq 3, we find that the general stress−strain constitutive law eq 2, based on entropic elasticity, remains valid in reinforced materials, in this range of strain amplitude (about 50%). This demonstrates that the predominant reinforcement mechanism in this range of strain amplitude is the local strain amplification in the bulk elastomer matrix. Note that downward shifts observed in critical strain at crystallization onset in reinforced materials are also generally interpreted as due to local strain amplification.[49]

The local strain amplification interpretation of reinforcement at large strain is directly evidenced by plotting the moduli against the slopes S_2 for all samples with different cross-link densities (Figure 6).

In the unfilled systems, evidently there is still a linear correlation between G' and S_2 with a small nonzero intercept

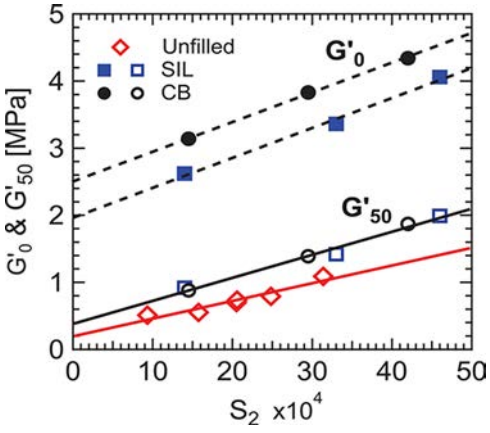

Figure 6. Storage shear moduli G'_0 (full symbols) and G'_{50} (empty symbols) for the 12 different studied samples, as a function of the slope S_2 of $\langle P_2 \rangle$ measured by X-ray scattering: unfilled (◊), SIL (□), and CB (○) samples.

on the modulus axis (corresponding to the nonzero intercept in Figure 4b). The value of the modulus extrapolated at $S_2 = 0$ is of order 2 to 5 × 10^5 Pa, which is coherent with a contribution of entanglements to modulus. In reinforced systems, G'_{50} still varies linearly with S_2 and the data are very close to that of pure systems. This illustrates that the increase of G'_{50} with respect to the pure systems (reinforcement at this strain amplitude) may be almost entirely interpreted as due to strain amplification already included in S_2 values. The small difference (constant upward shift of G'_{50} data in filled samples compared with unfilled ones) may be due to other mechanisms (which are at play at small amplitudes, see below) still contributing to G'_{50}. It could also be related to different mechanical histories: shear modulus is measured on as-prepared samples whereas the amorphous orientation parameter was measured on pre-stretched samples (3 cycles at 350%).

In the linear small strain ($\lesssim$ 0.1%) regime, G'_0 values are well above G'_{50} and do not vary proportionally to the slopes S_2 as the cross-link density varies. Thus, these values do not apparently follow the general constitutive law eq 2. Note again that this increase in G'_0 values is reversible.

5. DISCUSSION

It has been shown that the increase of shear modulus G'_{50} at medium/large strain amplitudes in the reinforced NR materials studied here may be almost entirely interpreted as due to strain amplification. Conversely, the modulus G'_0 in the low strain regime is much larger, and it is not proportional to the cross-link density neither to the chain segment orientational response S_2, indicating a breakdown of the general stress-optical law, eq 2, in this range of strain amplitudes.

The different reinforcement mechanisms presented in section 2.1 may now be discussed in the light of these experimental results. The increase of the G'_0 modulus might be related to an increase of the elastomer matrix modulus, related to some regions in the matrix with an effectively larger cross-link density, due, e.g., to enhanced topological constraints in the vicinity of filler surfaces.[9,10] In order to account for an increase of modulus by a factor of about 3 in the linear regime, assuming that an overall volume fraction 20% of the elastomer matrix (in the vicinity of fillers) would be affected, then the effective local cross-link density should typically be increased by a factor about 10−15, with this factor increasing even more as the affected volume fraction of the matrix would decrease. We have checked this possible local increase in cross-link density by NMR. Distributions of cross-link density in unfilled and filled samples are shown in Figure 7. Within the resolution of the experiment, we find that cross-link density distributions are the same in both unfilled and filled samples with same average ν value, as already reported in similar and other systems.[50,51] In Figure 7, we purposely show a large range of cross-link densities in abscissa, to illustrate that no contribution with increased cross-link density up to ten times the measured average value (which, on the examples shown, is about 3.5 × 10^{-4} mol·g^{-1}) is observed. Moreover, according to eq 3 and related discussion, a local increase in cross-link density would give an additional chain segment orientation, i.e. an increased slope in the $\langle P_2 \rangle$ vs $\lambda^2 - \lambda^{-1}$ curves at very small strain values, which is not observed (Figure 4a).

Let us now discuss the contribution from local shear associated with strong confinement (lubrication effects). It has been argued in section 2.1 that this effect would indeed give an amplified mechanical response G', relative to the orienta-

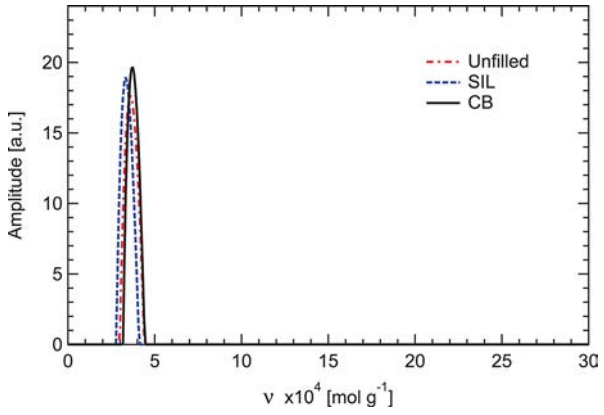

Figure 7. Distributions of cross-link density ν in a pure, unfilled NR sample (1.0 phr S) and in SIL and CB filled materials (1.5 phr S), which have roughly the same average values $\nu \approx 3.5 \times 10^{-4}$ mol·g^{-1}. No contribution from regions with cross-link densities up to 10 times the average value is observed.

tional response S_2. However, the effective modulus implied in this mechanism still involves the shear modulus, amplified with respect to the overall (macroscopic) modulus by a factor depending on local confinement, as discussed in section 2.1. Therefore, the associated overall (macroscopic) resulting modulus should still be proportional to the cross-link density, or, more precisely, G_0' values in Figure 6 should extrapolate to the roughly same ordinate as G_{S0}' values at S_2 values extrapolated to zero, contrary to what is observed. In other words, equivalently, it does not explain the extrapolated intercept at ≈2 MPa of G_0' as the cross-link density $\nu \to 0$. Thus, we argue that the amplification of the modulus G_0' should not be due to this mechanism.

Finally, the results reported here indicate that the extra reinforcement observed in the linear regime, which corresponds to a breakdown of the general elastomeric constitutive equation eq 3, is due to some *nonentropic* contribution to the stress–strain constitutive law. It demonstrates that part of the stress is supported by a percolating network of rigid or strongly confined component at small strain amplitude, and that this rigid network component is broken at large strain amplitude, the stress then being entirely supported by the elastomer matrix with an almost fully entropic response. This idea has been generally accepted already, based on indirect, model dependent analysis of mechanical data. The experiments presented here do not give direct evidence for a particular mechanism responsible for this rigid percolating network. We claim that we bring a new, direct experimental evidence of that in this work. These rigid elements may be either direct contacts between fillers, or glassy polymer bridges in between neighboring fillers. It is important to note again that these solid-like contributions to the mechanical response are reversible.

6. CONCLUSION

What has been shown here is that, at medium/large strain amplitudes, mechanical reinforcement observed in elastomers filled with carbon black or precipitated silica is mostly due to chain segment overorientation (or equivalently strain amplification) in the bulk elastomer matrix. This has been demonstrated quantitatively by correlating mechanical data to chain segment orientation measured by X-rays, taking into account the effective cross-link density measured by NMR. In the linear regime (small strain amplitudes), the larger increase of modulus is related to other, nonentropic (interfacial) reinforcement mechanisms, related to strong confinement, which are active even at the temperature studied here, corresponding to T_g + 120 K. It follows that, in the linear regime, the modulus is not proportional to the cross-link density of the matrix. Therefore, it cannot be expressed as a separable formula of the form $G_0' = G_{pure}'f(\Phi)$, with G_{pure}' the elastic modulus of the elastomer matrix (at the same cross-link density) and $f(\Phi)$ a reinforcement factor depending only on the reinforcing filler system, namely the volume fraction, structure, morphology and dispersion state of fillers. Thus, in the linear regime, the constitutive equation of the elastomer matrix cannot be considered to be unaffected by the presence of fillers. We may expect that these effects would be even more pronounced at lower temperature, when one enters a regime of higher mechanical reinforcement, i.e. closer to the maximum of the reinforcement curve as shows in Figure 1.

AUTHOR INFORMATION

Corresponding Author

E-mail: (P.S.) paul.sotta-exterieur@solvay.com.

Notes

The authors declare no competing financial interest.

ACKNOWLEDGMENTS

We thank B. Moreaux (Silica Solvay) for helping in the preparation of the samples and in the oscillatory shear measurements. We also thank Prof. Kay Saalwächter for fruitful discussions. R.P.-A. acknowledges the funding by the ANR Grant TaylRub 2009.

REFERENCES

(1) Heinrich, G.; Klüppel, M.; Vilgis, T. A. *Curr. Opin. Solid State Mater. Sci.* **2002**, *6*, 195–203.
(2) Pye, J. E.; Roth, C. B. *Phys. Rev. Lett.* **2011**, *107*, 235701.
(3) Wong, S.; Vaia, R. A.; Giannelis, E. P.; Zax, D. B. *Solid State Ionics* **1996**, *86–88*, 547–557.
(4) Mujtaba, A.; Keller, M.; Ilisch, S.; Radusch, H.-J.; Thurn-Albrecht, T.; Saalwächter, K.; Beiner, M. *Macromolecules* **2012**, *45*, 6504–6515.
(5) Wang, M. J. *Rubber Chem. Technol.* **1998**, *71*, 520–589.
(6) Medalia, A. I. *Rubber World* **1973**, *168*, 49.
(7) Payne, A. R. *J. Appl. Polym. Sci.* **1965**, *9*, 1073–1082.
(8) Sternstein, S. S.; Zhu, A.-J. *Macromolecules* **2002**, *35*, 7262–7273.
(9) Bogoslovov, R. B.; Roland, C. M.; Ellis, A. R.; Randall, A. M.; Robertson, C. G. *Macromolecules* **2008**, *41*, 1289–1296.
(10) Sternstein, S. S.; Amanuel, S.; Shofner, M. L. *Rubber Chem. Technol.* **2010**, *83*, 181–198.
(11) Reichert, W. F.; Göritz, D.; Duschl, E. J. *Polymer* **1993**, *34*, 1216–1221.
(12) Fukahori, Y. *Rubber Chem. Technol.* **2007**, *80*, 701–725.
(13) Maier, P. G.; Goeritz, D. *Kautsch. Gummi Kunstst.* **1996**, *49*, 18–21.
(14) Litvinov, V.; Orza, R.; Klüppel, M.; van Duin, M.; Magusin, P. *Macromolecules* **2011**, *44*, 4887–4900.
(15) Vladkov, M.; Barrat, J. L. *Macromolecules* **2007**, *40*, 3797–3804.
(16) Termonia, Y. *Polymer* **2010**, *51*, 4448–4451.
(17) Zhu, Z.; Thompson, T.; Wang, S.-Q.; von Meerwall, E. D.; Halasa, A. *Macromolecules* **2005**, *38*, 8816–8824.
(18) Akutagawa, K.; Yamaguchi, K.; Yamamoto, A.; Heguri, H.; Jinnai, H.; Shinbori, Y. *Rubber Chem. Technol.* **2008**, *81*, 182–189.
(19) Klüppel, M.; Schuster, R. H.; Heinrich, G. *Rubber Chem. Technol.* **1997**, *70*, 243–255.
(20) Litvinov, V. M.; Steeman, P. A. M. *Macromolecules* **1999**, *32*, 8476–8490.

(21) Berriot, J.; Montes, H.; Lequeux, F.; Long, D. R.; Sotta, P. *Macromolecules* **2002**, *35*, 9756−9762.
(22) Berriot, J.; Montes, H.; Lequeux, F.; Long, D. R.; Sotta, P. *Europhys. Lett.* **2003**, *64*, 50.
(23) Merabia, S.; Sotta, P.; Long, D. R. *Macromolecules* **2008**, *41*, 8252−8266.
(24) Dequidt, A.; Long, D. R.; Sotta, P.; Sanséau, O. *Eur. Phys. J. E* **2012**, *35*, 61−83.
(25) Berriot, J.; Lequeux, F.; Monnerie, L.; Montes, H.; Long, D. R.; Sotta, P. *J. Non-Cryst. Solids* **2002**, *307*, 719−724.
(26) Papon, A.; Montes, H.; Hanafi, M.; Lequeux, F.; Guy, L.; Saalwächter, K. *Phys. Rev. Lett.* **2012**, *108*, 065702.
(27) Robertson, C. G.; Lin, C. J.; Rackaitis, M.; Roland, C. M. *Macromolecules* **2008**, *41*, 2727−2731.
(28) Robertson, C. G.; Rackaitis, M. *Macromolecules* **2011**, *44*, 1177−1181.
(29) Vieyres, A.; Pérez-Aparicio, R.; Albouy, P.-A.; Sanseau, O.; Saalwächter, K.; Long, D. R.; Sotta, P. *Macromolecules* **2013**, *46*, 889−899.
(30) Treloar, L. R. G. *The Physics of Rubber Elasticity*; Clarendon Press: Oxford, England, 1975.
(31) Erman, B.; Mark, J. E. *Structures and Properties of Rubberlike Networks*; Oxford University Press: New York, 1997.
(32) Hyun, K.; Wilhelm, M.; Klein, C. O.; Cho, K. S.; Nam, J. G.; Ahn, K. H.; Lee, S. J.; Ewoldt, R. H.; McKinley, G. H. *Prog. Polym. Sci.* **2011**, *36*, 1697−1753.
(33) Guth, E.; Gold, O. *Phys. Rev.* **1938**, *53*, 322.
(34) Smallwood, H. M. *J. Appl. Phys.* **1944**, *15*, 758−766.
(35) Domurath, J.; Saphiannikova, M.; Ausias, G.; Heinrich, G. *J. Non-Newtonian Fluid Mech.* **2012**, *171*−*172*, 8−16.
(36) Doi, M.; Edwards, S. F. *The Theory of Polymer Dynamics*; Oxford University Press: New York, 1988.
(37) Flory, P. J. *Statistical Mechanics of Chain Molecules*; Interscience: New York, 1969.
(38) Fredrickson, G. H.; Ajdari, A.; Leibler, L.; Carton, J.-P. *Macromolecules* **1992**, *25*, 2882−2889.
(39) Batchelor, G. K. *An Introduction to Fluid Dynamics*; Cambridge University Press: Cambridge, U.K., 2000.
(40) Guyon, E.; Hulin, J.-P.; Petit, L.; Mitescu, C. D. *Physical Hydrodynamics*; Oxford University Press: Oxford, U.K., 2001.
(41) Johnson, K. L. *Contact Mechanics*; Cambridge University Press: Cambridge, U.K., 1985.
(42) Mitchell, G. R. *Polymer* **1984**, *25*, 1562−1572.
(43) Albouy, P.-A.; Guillier, G.; Petermann, D.; Vieyres, A.; Sanseau, O.; Sotta, P. *Polymer* **2012**, *53*, 3313−3324.
(44) Saalwächter, K. *Prog. Nucl. Magn. Reson. Spectrosc.* **2007**, *51*, 1−35.
(45) Cohen-Addad, J. P. *J. Chem. Phys.* **1974**, *60*, 2440−2453.
(46) Saalwächter, K.; Herrero, B.; López-Manchado, M. A. *Macromolecules* **2005**, *38*, 9650−9660.
(47) Chassé, W.; López Valentn, J.; Genesky, G. D.; Cohen, C.; Saalwächter, K. *J. Chem. Phys.* **2011**, *134*, 044907.
(48) Pérez-Aparicio, R.; Schiewek, M.; López Valentín, J.; Schneider, H.; Long, D. R.; Saphiannikova, M.; Sotta, P.; Saalwächter, K.; Ott, M. *Macromolecules* **2013**, *46*, 5549−5560.
(49) Dupres, S.; Long, D. R.; Albouy, P.-A.; Sotta, P. *Macromolecules* **2009**, *42*, 2634−2644.
(50) López Valentín, J.; Mora-Barrantes, I.; Carretero-González, J.; López-Manchado, M.; Sotta, P.; Long, D. R.; Saalwächter, K. *Macromolecules* **2010**, *43*, 334−346.
(51) Saalwächter, K. *Rubber Chem. Technol.* **2012**, *85*, 350−386.